博 士 論 文

Immunolocalization of FGF23 in bone metastasis of human breast carcinoma MDA231 cells
(乳がん MDA231 細胞の骨転移巣における FGF23 の免疫局在について)

平成３１年　３月申請

北海道大学
大学院歯学研究科口腔医学専攻

横　山　亜　矢　子

.

Immunolocalization of FGF23 in bone metastasis of human breast carcinoma MDA231 cells

Ayako Yokoyama

Gerodontology, Department of Oral Health Science, Graduate School of Dental Medicine, Hokkaido University, Sapporo, Japan

Running title: FGF23 synthesis in osteolytic metastasis.

§ **Address for correspondence to**

Ayako Yokoyama

Gerodontology, Department pf Oral Health Science,

Graduate School of Dental Medicine,

Hokkaido University

Kita-13, Nishi-7, Kita-Ku, Sapporo, Japan

Tel/Fax: +81-11-706-4226

E-mail: ayako.y@den.hokudai.ac.jp

Abstract

After the onset of bone metastasis, the tumor cells appear to make surrounding microenvironments, including systemic and local serum concentrations of inorganic phosphate (Pi), suitable for their proliferation, matrix degradation, and nest expansion. In this study, we attempted to clarify if bone-metastasized tumors affect the localization of serum Pi concentration regulatory factors. Using femoral metastatic lesions of BALB/c nu/nu mice at one month after the intracardiac injection of human breast carcinoma MDA231 cells, we examined the immunolocalization of fibroblast growth factor (FGF) 23 and FGFR1/αklotho, which are involved in regulating serum concentration of Pi by cooperating with kidney, and of ectonucleotide pyrophosphatase/phosphodiesterase 1 (ENPP1), tissue nonspecific alkaline phosphatase (TNALP), and PHOSPHO1, which regulate the local synthesis of Pi. In the metastatic lesions of femoral metaphyses, many tartrate-resistant acid phosphatase (TRAP)-positive osteoclasts accumulated on osteopontin-reactive scalloped trabecular surfaces, indicating active osteolytic metastasis. Although MDA231 cells showed very weak FGF23 immunoreactivity when cultured *in vitro*, MDA231 cells revealed intense FGF23 -reactivity in the metastasized lesions. Despite significantly- elevated serum FGF23 levels, there was no significant decrease in the serum concentration of Pi in nu/nu mice with bone-metastasized tumor when compared with the control mice and mice injected with MDA231 cells in mammary glands. Interestingly, FGF23 was abundantly synthesized in the bone-metastasized MDA231 cells, while osteocytes in bone adjacent to the FGF23-immunopositive tumor nests were negative for FGF23. Unlike the reduced synthesis of FGF23 in osteocytes, the osteocytes proximal to MDA231 cells were shown to synthesize dentin matrix protein (DMP)-1. Therefore, it seems possible that the abundant FGF23 secreted by MDA231 cells inhibits the surrounding osteocytes from synthesizing FGF23. In addition, immunopositivity of ENPP1 but not TNALP or PHOSPHO1 was broadly seen mainly in fibroblastic stromal cells in metastatic lesions, indicating that ENPP1 would be useful for bone-metastasized MDA231 cells. Taken together, it seems likely that rather than affecting the serum concentration of Pi, FGF23 plays some local roles in establishing suitable conditions favoring the metastasis of MDA231 cells in the bone in an autocrine/paracrine manner.

333 words

Key words: ***bone metastasis, FGF23, MDA231 cell, osteocyte, ENPP1***

.

Introduction

Bone metastasis is an important clinical condition in patients suffering from a malignant tumor, and blood circulation seems to be the medium for tumor cells to spread and establish metastatic lesions. Over a hundred years ago, Stephen Paget[1)] proposed the "seed and soil" hypothesis, stating that "seeds" of metastatic breast cancer cells preferentially migrate to the "soil" of the bone matrix. Bone-metastasized tumors show osteolytic, osteogenic, or combined lesions depending on the interaction between tumor cells and bone cells. Animal models mimicking bone metastasis have been established to elucidate the intrinsic pathological events of bone metastasis using cancer cell lines. Breast carcinomas are the most common tumors to cause osteolytic lesions, and MDA231 cells of human breast carcinoma selectively colonize the femur and tibia of nu/nu mice, thus inducing osteolytic metastasis[2-4)].

Among the various adverse events associated with osteolytic metastasis, such as bone pain, numbness, paralysis, bone fractures, and hypercalcemia, hypercalcemia is well known to worsen the patient condition by inducing nausea, vomiting, and consciousness disorder[5)]. Tumor-induced osteomalacia/hypophosphatemia (TIO) was reported as an adverse event suggested to be caused by fibroblast growth factor 23 (FGF23) secreted by the tumors[2, 6-8)]. When a diagnosis TIO is suspected, FGF23-secreting tumors are expected to be present in patients; however, these tumors are often small, slow growing, and benign with mesenchymal origin[9-11)]. In a normal state, FGF23 is well known to be mainly synthesized by osteocytes[12, 13)] and is circulated to reach the kidney. FGF23 binds the receptor complex of FGFR1c/αklotho in the proximal renal tubules to inhibit phosphate reabsorption by sodium phosphate co-transporter type IIa/IIc, consequently reducing the serum concentration of inorganic phosphate (Pi)[14-18)]. It would be interesting to know the purpose for which the tumors secrete FGF23 in bone metastasis. In this context, the following unknown aspects are of particular interest: 1) whether the resultant hypophosphatemia induced by the tumor-derived FGF23 is beneficial for the tumor growth and expansion of their nests, 2) whether the FGF23 secreted by the tumors affects the stromal cells or tumor cells themselves in tumor nests in an autocrine/paracrine manner, and 3) whether TIO is merely a side effect of the abundantly synthesized FGF23 by the tumors. If hypophosphatemia is beneficial for tumor proliferation, matrix degradation, and their invasion into the surrounding tissues, not only FGF23 but also 1) membrane transports and enzymes involved in the regulation of local concentration of Pi, such as tissue-nonspecific alkaline phosphatase (TNALP)[19-21)],

.

2) ectonucleotide pyrophosphatase/phosphodiesterase family member 1 (ENPP1; a membrane-bound glycoprotein that regulates bone mineralization by hydrolyzing extracellular nucleotide triphosphates to produce pyrophosphates)[22], 3) and PHOSPHO1[23-25] would be beneficial for tumor growth; therefore, tumor cells may affect the localization of ENPP1, TNALP, and PHOSPHO1 after the onset of bone metastasis.

In this study, we have attempted to examine the immunolocalization of FGF23, αklotho and FGFR1, all of which are involved in the systemic regulation of serum concentration of Pi by cooperating with kidney. Further, we examined the local regulators of Pi supply, such as TNALP, ENPP1, and PHOSPHO1, in metastatic lesions populated by MDA231 cells in the femora of BALB/c nu/nu mice.

.

Materials and Methods

Tissue preparation for histological examination

All animal experiments were conducted under the Guidelines for Animal Experimentation of Hokkaido University (approval No.16-0031). Human breast carcinoma MDA231 cells (American Type Culture Collection, Rockville, MD, USA) were cultured in α-minimum essential medium (αMEM, Flow Laboratories, Irvine, Scotland) supplemented with heat-inactivated 10% fetal bovine serum (FBS, Cosmo Bio. Co. Ltd., Tokyo, Japan) at 37 ˚C in a humidified atmosphere of 5% CO_2. As previously reported[2, 3, 26], MDA231 cells (10^5 cells per mouse) were injected using a 22 gauge needle into the left cardiac ventricle of 5-6 week-old BALB/c nu/nu mice (CLEA Japan Co. Ltd, Tokyo) under anesthesia with an intraperitoneal injection of sodium pentobarbital (n=5). The same quantity of MDA231 cells was subcutaneously injected in the region of mammary glands of age-matched BALB/c nu/nu mice (n=5). For control experiments, only Ringer's solution was injected into the left cardiac ventricle (n=5). After 4 weeks, femora of the treated- mice were taken for soft X-ray examination (SOFRON Ltd, Tokyo, Japan). The mice having bone metastasis, those having developed tumor mass in the mammary glands, and control mice were anesthetized with an intraperitoneal injection of sodium pentobarbital, and their blood samples were collected through cardiac ventricles to measure the concentration of serum calcium (Ca), Pi, and FGF23. Thereafter, the mice were perfused with 4% paraformaldehyde diluted in a 0.1M phosphate buffer (pH 7.4), and the femora were removed and immersed in the same fixative for 24 h at 4 °C for histochemical examination[27]. The specimens for histochemistry were then decalcified with 10% ethylenediamine tetraacetic disodium salt (EDTA-2Na) solution and dehydrated with increasing concentrations of ethanol before paraffin embedding.

Immunohistochemistry for dentine matrix protein (DMP)-1, sclerostin, FGF23, FGFR1, αklotho, TNALP, ENPP1, and PHOSPHO1 in the metastatic lesion of nu/nu femora

After the inhibition of endogenous peroxidase activity with methanol containing 0.3% hydrogen peroxidase for 30 min, dewaxed paraffin sections were pretreated with 1% bovine serum albumin (BSA; Seologicals Proteins Inc. Kankakee, IL) in PBS (1% BSA-PBS) for 30 min. The histological sections were incubated with either rabbit antibody against DMP-1 (Takara Bio Inc., Otsu, Japan) at a dilution of 1:500 overnight at 4 °C or rabbit antisera against TNALP[19] at a dilution of 1:300 at room temperature (RT); then they were reacted with horseradish peroxidase (HRP)-conjugated goat anti-

rabbit IgG (DakoCytomation, Glostrup, Denmark) at a dilution of 1:100 for 1 h. For the detection of ENPP1, the sections were incubated with goat polyclonal anti-ENPP1 (Everest Biotech Ltd., Oxfordshire, UK) at a dilution of 1:200 for 1 h followed by incubation with HRP-conjugated rabbit anti-goat IgG (American Qualex Scientific Products, Inc., San Clemente, CA). Regarding FGF23/FGFR1/αklotho axis, the histological sections were incubated with mouse anti-FGF23 (R&D systems, Inc., Minneapolis, MN) at a dilution of 1:100 for 2 h, or mouse monoclonal anti-FGFR1 (Abcam plc., Cambridge, UK) at a dilution of 1:25 for 1 h. These sections were then reacted with HRP-conjugated rabbit anti-mouse IgG (Invitrogen Co., Camarillo, CA) at a dilution of 1:100 for 1 h. For the detection of αklotho, the sections were incubated with rat monoclonal anti-mouse klotho antibody (Thermo Fisher Scientific Ltd., Waitham, MA) at a dilution of 1:50 for 2h, and then, they were reacted with HRP-conjugated rabbit anti-rat IgG. Regarding the immunodetection of PHOSPHO1, after incubating with human monoclonal anti-PHOSPHO1 (Bio-Rad Laboratories Inc., Hercules, CA) at a dilution of 1:100, the sections were reacted with rabbit anti-myc Tag (Medical & Biological Laboratories Co., Ltd., Nagoya, Japan) and then with HRP-conjugated swine anti-rabbit IgG (DakoCytomation) at a dilution of 1:100. For the visualization of all immunoreactions, diaminobenzidine tetrahydrochloride (DAB) was employed as a substrate. All sections were counterstained with methyl green and observed under a light microscope (Eclipse E800, Nikon Instruments Inc. Tokyo, Japan).

Double detection of tartrate-resistant acid phosphatase (TRAP) and osteopontin

After the treatment with 0.3% hydrogen peroxidase and 1% BSA–PBS, the sections were incubated with rabbit anti-osteopontin antisera (Cosmo Bio, Co., Ltd., Tokyo, Japan) at a dilution of 1:2000 for 1 h, followed by incubation with HRP-conjugated goat anti-rabbit IgG (DakoCytomation). The immunoreacted sections were subjected to the detection of TRAP enzymatic activity as previously described[28]; briefly, slides were rinsed with PBS and incubated in a mixture of 2.5 mg of naphthol AS-BI phosphate (Sigma-Aldrich Co. LLC, St. Louis, MS), 18 mg of Red Violet LB (Sigma-Aldrich) salt, and 100 mM L(+)-tartaric acid (0.76 g, Nacalai Tesque, Inc., Kyoto, Japan) diluted in 30 mL of 0.1 M sodium acetate buffer (pH 5.0) for 15 min at 37 °C.

Immunocytochemistry of FGF23 on cultured MDA231 cells

MDA231 cells were cultured on glass coverslips in dishes with 3.5 cm diameter containing αMEM

supplemented with heat-inactivated 10% FBS before immunocytochemistry of FGF23. The specimens were fixed with 4% paraformaldehyde in a 0.1 M phosphate buffer (pH 7.4) for 2 h at RT. The specimens were rinsed with PBS several times and then treated with 1% BSA–PBS for 10 min. They were then incubated with mouse anti-FGF23 (R&D systems) at a dilution of 1:100 for 2 h, and then with HRP-conjugated rabbit anti-mouse IgG (Invitrogen) at a dilution of 1:100 for 1 h. For visualization of the immunoreaction, DAB was employed as a substrate, and the specimens were faintly counterstained with methyl green before observation under a light microscope.

Measurement of serum FGF23, Ca, and Pi

Blood samples were obtained from all mice that showed bone metastasis g, that had MDA231 cells injected in the mammary gland, and controls (n=5 each) before perfusion. Serum samples were stored at - 30 ˚C before performing the assays. Serum levels of Ca and Pi were quantified by Oriental Yeast Co., Ltd. Serum intact FGF23 was quantified using the sandwich ELISA kits (Kainos Laboratories, Tokyo, Japan) as previously reported[29]. All assays were performed in accordance with the manufacturers' instructions.

Statistical analysis

All statistical analyses were assessed by one-way ANOVA followed by the Tukey–Kramer multiple comparisons test, and all values are presented as mean ± standard deviation as reported previously[30]. Values of $p < 0.05$ were considered statistically significant.

.

Results

Osteolytic bone metastasis by MDA231 cells

Soft X-ray analysis revealed relatively-broad translucent areas representing a metastatic lesion in the metaphyses of both the left and right femora and tibiae of nu/nu mice **(Fig. 1)**. Consistent with soft X-ray analysis, the histological observation revealed huge masses of metastasized MDA231 cells in the femoral metaphyses along with few trabeculae extending from the growth plates **(Figs. 2a, b)**. The metastasized tumor nests had a higher cell density than the surrounding bone marrow. In tumor nests, there were only a few fragmented trabeculae featuring intense osteopontin-reactive scalloped trabecular surface, which localized many TRAP-positive osteoclasts **(Figs. 2c, d)**.

FGF23 immunolocalization in the metastatic lesion and the neighboring cortical bone

The cultured MDA231 cells showed weak FGF23 immunoreactivity *in vitro* as shown in **Fig. 3a**. However, after the onset of bone metastasis, tumor nests metastasized in the femoral metaphyses demonstrated intense FGF23 immunoreactivity **(Fig. 3b)**. Interestingly, the trabeculae surrounded by the metastasized MDA231 cells showed little FGF23-immunoreactivity in osteocytes, while trabeculae distant from the metastatic lesion possessed FGF23-immmunopositive osteocytes **(Compare Figs. 3c and d)**. The histological sections showed many intact osteocytes in the cortical bone adjacent to tumor nests, except those in the superficial layer of the cortical bone. Several empty lacunae could be seen in the superficial layer proximal to tumor nests, whereas many intact osteocytic lacunae were present in the inner portion of the cortical bone **(Figs. 3e, f)**. Osteocytes in the cortical bone adjacent to the metastasized tumor nests hardly showed FGF23 immunoreactivity, whereas those distant from the metastatic lesion showed intense FGF23 immunoreactivity **(Compare Figs. 3c and d)**. Unlike FGF23 and DMP-1 －another molecule abundantly expressed in osteocytes[28, 31, 32)], were observed in the osteocytes of the cortical bone adjacent to the metastasized tumor nests **(Figs. 3i, f)**.

Serum concentration of Ca, Pi, and FGF23 and the immunolocalization of FGFR1 and αklotho in the metastatic lesion

Mice with bone metastasis showed significantly higher serum FGF23 levels than mice subcutaneously injected with MDA231 cells (385.87 $\pm$ 58.99pg/mL vs 229.65 $\pm$ 8.73 pg/mL, $p<0.05$) and control mice without injection of tumor cells (385.87 $\pm$ 58.99 pg/mL vs 155.90 $\pm$ 18.17 pg/mL, $p<0.01$) **(Fig.**

.

4a). Despite the increased index of serum FGF23, there was no significant difference in serum Ca levels among the mice bone-metastasized tumor (7.90 ± 0.22 mg/dL), the mice with subcutaneous injection of tumor cells (8.36 ± 0.26 mg/dL) and the control mice (7.82 ± 0.13 mg/dL) **(Fig. 4b).** Similarly, there was no significant difference in serum Pi levels among the mice bone-metastasized tumor (8.30 ± 0.58 mg/dL), the mice with subcutaneous injection of tumors (8.62 ± 0.61 mg/dL), and the control mice (8.20 ± 0.46 mg/dL) **(Fig. 4c)**. Since bone-metastasized MDA231 cells did not affect the serum concentration of Pi, we have examined the possibility that FGF23 secreted by the tumor cells affects the cells themselves in an autocrine/paracrine manner. Our immunohistochemistry showed FGFR1-immunoreactive fibroblastic stromal cells extending their cytoplasmic processes rather than cuboidal tumor cells **(Figs. 5a, b)**, and some fibroblastic stromal cells in tumor nests exhibited a weak immunoreactivity of αklotho **(Fig. 5c)**.

Immunolocalization of ENPP1, TNALP, and PHOSPHO1 in the metastasized lesion

We also examined ENPP1, TNALP, and PHOSPHO1, all of which are involved in the local synthesis of monophosphates and pyrophosphates. Metastasized tumor nests showed intense ENPP1 -immunopositivity mainly in fibroblastic stromal cells and slightly in cuboidal tumor cells **(Figs. 5d, g)**. However, TNALP -immunoreactivity was observed in osteoblasts localized on the trabecular surfaces but was never seen inside tumor nests **(Figs. 5e, h)**. PHOSPHO1 -immunopositivity was detected in osteoblasts located on the endosteal surfaces of cortical bone, but not in tumor nests **(Figs. 5f, i)**.

.

Discussion

To our knowledge, this is the first report that demonstrates that when closely surrounded by FGF23-secreting MDA231 cells, the synthesis of FGF23 by osteocytes in the cortical bone is inhibited as shown in **Fig. 3**. Unlike the reduced synthesis of FGF23, the osteocytes proximal to the metastasized MDA231 cells synthesized DMP-1. Therefore, it seems possible that abundant FGF23 produced by the metastasized MDA231 cells inhibits the surrounding osteocytes from secreting FGF23. Although MDA231 cells cultivated *in vitro* showed slight FGF23 synthesis, after the onset of bone metastasis, they synthesized FGF23 abundantly. Pro-inflammatory stimuli are reportedly capable of increasing osteocyte secretion of FGF23[33]. Taken together, it seems likely that FGF23 secreted by MDA231 cells supports bone metastasis and its expansion after the onset of the metastasis and affects the surrounding pre-existing osteocytes to inhibit FGF23 synthesis. Thus, FGF23 secreted by MDA231 cells may play a role in establishing suitable circumstances for bone tumor.

Next, we wondered whether abundant FGF23 produced by MDA231 cells would reduce the serum concentration of Pi and if the resultantly-deceased concentration of Pi would provide adequate circumstances for bone metastasis of MDA231 cells or whether abundant FGF23 would locally and directly affect MDA231 cells and the surrounding cells to alter the histological circumstances to make them adequate for the tumor growth in the bone. To address this issue, we measured the serum concentrations of FGF23, Ca, and Pi, and as a consequence, despite the elevated index of FGF23, the concentration of Ca and Pi did not significantly change as shown in **Fig. 4**. No significant decrease in serum Pi levels may be due to the increased concentration of FGF23 secreted by MDA231 cells (2.5 times higher than the control specimens). However, it was not enough for markedly-reduced concentration of serum Pi in mice, or FGF23 secreted by the tumor cells may be subjected to being immediately processed at the C-terminus of this molecule, before reaching the kidney[34, 35]. Therefore, our animal study does not seem to mimic recently- reported TIO[2, 6-8]. Taken together, FGF23 secretion by metastasized MDA231 cells does not appear to be directed to reduce the serum concentration of Pi but may be related to the local action of FGF23 in the metastatic lesion *in situ*. If so, it is likely that FGF23 secreted by MDA231 cells locally affects the tumors and the surrounding cells in an autocrine/paracrine manner. Our observation revealed the immunoreactivity of FGFR1/αklotho mainly in fibroblastic stromal cells inside tumor nests rather than in cuboidal tumor

cells, as shown in **Fig. 5**. Therefore, we assume that FGF23 secreted by the MDA 231 cells may function on fibroblastic stromal cells in the metastasized lesions as it has been reported that stromal cells in tumor nests interact with the tumor cells. However, the nature and medium of the effect FGF23 has on the tumor and neighboring stromal cells remains unknown.

We have finally examined ENPP1, TNALP, and PHOSPHO1, all of which are involved in the regulation of local synthesis of pyrophosphates and Pi. Consequently, the immunolocalization of TNALP and PHOSPHO1 was to that seen in normal bone tissues, *i.e.*, TNALP and PHOSPHO1 were mainly localized in the osteoblasts on the fragmented trabeculae. In contrast, many fibroblastic stromal cells and tumor cells were intensely ENPP1-immunoreactive, indicating abundant synthesis of inorganic pyrophosphates, which inhibit mineralization in the bone[20, 36]. However, except the biological function of synthesizing pyrophosphates in the bone, ENPP1 reportedly serves as a facilitator of breast cancer bone metastasis[37] and plays an important role in balancing the pool of nucleotides, maintaining glioblastoma stem-like cells in an undifferentiated proliferative state[38]. Further, it is also associated with the increased risk of glucose intolerance and type II diabetes[39]. Thus, ENPP1 possibly plays a role in facilitating tumor malignancy and maintaining tumor stem cells in the metastasized lesion of MDA231 cells. However, further study is necessary to clarify the pathological function of ENPP1 in the bone-metastasized lesion of tumor cells.

Concluding Remarks

This study using an animal model of bone metastasis demonstrated that the osteocytes in the cortical bone were inhibited to synthesize FGF23, when closely surrounded by FGF23-secreting MDA231 cells, indicating a pivotal role of tumor-derived FGF23 in establishing suitable circumstances for tumors in the bone.

.

Acknowledgements

This study was partially supported by the Grants-in Aid for Scientific Research of JSPS (Hasegawa T and Amizuka N), and Promoting International Joint Research (Bilateral Collaborations) of JSPS in Japan and NSFC in China (Amizuka N and Li M).

Conflict of interest

No potential conflicts of interest exist.

.

References

1. Paget S: The distribution of secondary growths in cancer mof the breast. Lancet 133: 571-573, 1889.

2. Shimamura T, Amizuka N, Li M, Luiz de Freitas PH, White JH, Henderson JE, Shingaki S, Nakajima T, Ozawa H: Histological observations on the microenvironment of osteolytic bone metastasis by breast carcinoma cell line. Biomed Res 26: 159–172, 2005.

3. Hiraga T, Nakajima T, Ozawa H: Bone resorption induced by a metastatic human melanoma cell line. Bone 16: 349–356, 1995.

4. Yoneda T, Sasaki A, Mundy GR: Osteolytic bone metastasis in breast cancer. Breast Cancer Res Treat. 32, 73–84, 1994.

5. Seccareccia D: Cancer-related hypercalcemia. Can Fam Physician 56: 244–246, 2010.

6. The ADHR Consortium: Autosomal dominant hypophosphataemic rickets is associated with mutations in FGF23. Nature Genetics 26: 345–348, 2000.

7. Shimada T, Mizutani S, Muto T, Yoneya T, Hino R, Takeda S, Takeuchi Y, Fujita T, Fukumoto S, Yamashita T: Cloning and characterization of FGF23 as a causative factor of tumor-induced osteomalacia. Proc Natl Acad Sci USA 98: 6500–6505, 2001.

8. Yamazaki Y, Okazaki R, Shibata M, Hasegawa Y, Satoh K, Tajima T, Takeuchi Y, Fujita T, Nakahara K, Yamashita T, Fukumoto S: Increased Circulatory Level of Biologically Active Full-Length FGF-23 in Patients with Hypophosphatemic Rickets/Osteomalacia. J Clin Endocrinol Metab 87: 4957–4960, 2002.

9. Folpe AL, Fanburg-Smith JC, Billings SD, Bisceglia M, Bertoni F, Cho JY, Econs MJ, Inwards CY, Jan de Beur SM, Mentzel T, Montgomery E, Michal M, Miettinen M, Mills SE, Reith JD, O'Connell JX, Rosenberg AE, Rubin BP, Sweet DE, Vinh TN, Wold LE, Wehrli BM, White KE,

Zaino RJ, Weiss SW: Most osteomalacia-associated mesenchymal tumors are a single histopathologic entity: an analysis of 32 cases and a comprehensive review of the literature. Am J Surg Pathol 28: 1–30, 2004.

10. Jiang Y, Xia WB, Xing XP, Silva BC, Li M, Wang O, Zhang HB, Li F, Jing HL, Zhong DR, Jin J, Gao P, Zhou L, Qi F, Yu W, Bilezikian JP, Meng XW: Tumor-induced osteomalacia: an important cause of adult-onset hypophosphatemic osteomalacia in China: Report of 39 cases and review of the literature. J Bone Miner Res 27: 1967–1975, 2012.

11. Chong WH, Andreopoulou P, Chen CC, Reynolds J, Guthrie L, Kelly M, Gafni RI, Bhattacharyya N, Boyce AM, El-Maouche D, Crespo DO, Sherry R, Chang R, Wodajo FM, Kletter GB, Dwyer A,Collins MT: Tumor localization and biochemical response to cure in tumor-induced osteomalacia. J Bone Miner Res 28: 1386–1398, 2013.

12. Ubaidus S, Li M, Sultana S, Luiz de Freitas PH, Oda K, Maeda T, Takagi R, Amizuka N: FGF23 is mainly synthesized by osteocytes in the regularly distributed osteocytic lacunar canalicular system established after physiological bone remodeling. J Electron Microsc (Tokyo) 58: 381–392, 2009.

13. Martin A, Liu S, David V, Li H, Karydis A, Feng JQ, Quarles LD: Bone proteins PHEX and DMP1 regulate fibroblastic growth factor Fgf23 expression in osteocytes through a common pathway involving FGF receptor (FGFR) signaling. FASEB J 25: 2551–2562, 2011.

14. Kurosu H, Ogawa Y, Miyoshi M, Yamamoto M, Nandi A, Rosenblatt KP, Baum MG, Schiavi S, Hu MC, Moe OW, Kuro-o M: Regulation of fibroblast growth factor-23 signaling by klotho. J Biol Chem 281: 6120–6123, 2006.

15. Nakatani T, Sarraj B, Ohnishi M, Densmore MJ, Taguchi T, Goetz R, Mohammadi M, Lanske B, Razzaque MS: In vivo genetic evidence for klotho-dependent, fibroblast growth factor 23 (Fgf23)-mediated regulation of systemic phosphate homeostasis. FASEB J 23: 433–441, 2009.

.

16. Urakawa I, Yamazaki Y, Shimada T, Iijima K, Hasegawa H, Okawa K, Fujita T, Fukumoto S, Yamashita T: Klotho converts canonical FGF receptor into a specific receptor for FGF23. Nature 444: 770–777, 2006.

17. Nabeshima Y: Toward a better understanding of Klotho. Sci Aging Knowledge Environ 2006: 11, 2006.

18. Hasegawa T, Sasaki M, Yamada T, Ookido I, Yamamoto T, Hongo H, Yamamoto T, Oda K, Yokoyama K, Amizuka N: Histochemical examination of vascular medial calcification of aorta in klotho-deficient mice. J Oral Biosciences 55: 10–15, 2013.

19. Oda K, Amaya Y, Fukushi-Irie M, Kinameri Y, Ohsuye K, Kubota I, Fujimura S, Kobayashi J: A general method for rapid purification of soluble versions of glycosylphosphatidylinositol-anchored proteins expressed in insect cells: an application for human tissue-nonspecific alkaline phosphatase. J Biochem 126: 694–699, 1999.

20. Hasegawa T: Ultrastructure and biological function of matrix vesicles in bone mineralization. Histochem Cell Biol 149: 289–304, 2018.

21. Amizuka N, Hasegawa T, Oda K, Luiz de Freitas PH, Hoshi K, Li M, Ozawa H: Histology of epiphyseal cartilage calcification and endochondral ossification. Front Biosci (Elite Ed): 2085–2100, 2012.

22. Huang R, Rosenbach M, Vaughn R, Provvedini D, Rebbe N, Hickman S, Goding J, Terkeltaub R: Expression of the murine plasma cell nucleotide pyrophosphohydrolase PC-1 is shared by human liver, bone, and cartilage cells. Regulation of PC-1 expression in osteosarcoma cells by transforming growth factor-beta. J Clin Invest 94: 560–567,1994.

23. Ciancaglini P, Yadav MC, Simão AM, Narisawa S, Pizauro JM, Farquharson C, Hoylaerts MF, Millán JL: Kinetic analysis of substrate utilization by native and TNAP-, NPP1-, or PHOSPHO1-deficient matrix vesicles. J Bone Miner Res 25:716–723, 2010.

.

24. Roberts S, Narisawa S, Harmey D, Millán JL, Farquharson C. Functional involvement of PHOSPHO1 in matrix vesicle-mediated skeletal mineralization. J Bone Miner Res 22: 617–627, 2007.

25. Stewart AJ, Roberts SJ, Seawright E, Davey MG, Fleming RH, Farquharson C. The presence of PHOSPHO1 in matrix vesicles and its developmental expression prior to skeletal mineralization. Bone 39:1000–1007, 2006.

26. Arguello F, Baggs RB, Frantz CN: A murine model of experimental metastasis to bone and bone marrow. Cancer Res 48: 6876–6881, 1988.

27. Hasegawa T, Endo T, Tsuchiya E, Kudo A, Shen Zhao, Moritani Y, Abe M, Yamamoto T, Hongo H, Tsuboi K, Yoshida T, Nagai T, Khadiza N, Yokoyama A, Luiz de Freitas PH, Li M, Amizuka N: Biological application of focus ion beam-scanning electron microscopy (FIB-SEM) to the imaging of cartilaginous fibrils and osteoblastic cytoplasmic processes. J Oral Biosciences 59: 55–62, 2017.

28. Hasegawa T, Amizuka N, Yamada T, Liu Z, Miyamoto Y, Yamamoto T, Sasaki M, Hongo H, Suzuki R, de Luiz de Freitas PH, Yamamoto T, Oda K, Li M: Sclerostin is differently immunolocalized in metaphyseal trabecules and cortical bones of mouse tibiae. Biomed Res 34: 153–159, 2013.

29. Imanishi Y, Hashimoto J, Ando W, Kobayashi K, Ueda T, Nagata Y, Miyauchi A, Koyano HM, Kaji H, Saito T, Oba K, Komatsu Y, Morioka T, Mori K, Miki T, Inaba M: Matrix extracellular phosphoglycoprotein is expressed in causative tumors of oncogenic osteomalacia. J Bone Miner Metab 30: 93–99, 2012.

30. Yamamoto T, Hasegawa T, Sasaki M, Hongo H, Tsuboi K, Shimizu T, Ota M, Haraguchi M, Takahata M, Oda K, Luiz de Freitas PH, Takakura A, Takao-Kawabata R, Isogai Y, Amizuka N: Frequency of Teriparatide Administration Affects the Histological Pattern of Bone Formation in Young Adult Male Mice. Endocrinology 157: 2604–2620, 2016.

31. Toyosawa S, Shintani S, Fujiwara T, Ooshima T, Sato A, Ijuhin N, Komori T: Dentin matrix protein 1 is predominantly expressed in chicken and rat osteocytes but not in osteoblasts. J Bone Miner Res 16: 2017–2026, 2001.

32. Winkler DG, Sutherland MK, Geoghegan JC, Yu C, Hayes T, Skonier JE, Shpektor D, Jonas M, Kovacevich BR, Staehling-Hampton K, Appleby M, Brunkow ME, Latham JA: Osteocyte control of bone formation via sclerostin, a novel BMP antagonist. EMBO J 22: 6267–6276, 2003.

33. Ito N, Wijenayaka AR, Prideaux M, Kogawa M, Ormsby RT, Evdokiou A, Bonewald LF, Findlay DM, Atkins GJ: Regulation of FGF23 expression in IDG-SW3 osteocytes and human bone by pro-inflammatory stimuli. Mol Cell Endocrinol 399: 208–218, 2015.

34. Benet-Pagès A, Lorenz-Depiereux B, Zischka H, White KE, Econs MJ, Strom TM: FGF23 is processed by proprotein convertases but not by PHEX. Bone 35: 455–462, 2004.

35. Shimada T, Muto T, Urakawa I, Yoneya T, Yamazaki Y, Okawa K, Takeuchi Y, Fujita T, Fukumoto S, Yamashita T: Mutant FGF-23 responsible for autosomal dominant hypophosphatemic rickets is resistant to proteolytic cleavage and causes hypophosphatemia in vivo. Endocrinology 143:3179–3182, 2002.

36. Fleisch H, Russell RG, Straumann F: Effect of pyrophosphate on hydroxyapatite and its implications in calcium homeostasis. Nature 212: 901–903, 1966.

37. Lau WM, Doucet M, Stadel R, HuangD, Weber KL, Kominsky SL: Enpp1: A Potential Facilitator of Breast Cancer Bone Metastasis. PLOS 8: e66752, 2013

38. Bageritz J, Goidts V: Functional characterization of ENPP1 reveals a link between cell cycle progression and stem-like phenotype in glioblastoma. Mol Cell Oncol 1: e964028, 2014.

39. Meyre D, Bouatia-Naji N, Tounian A, Samson C, Lecoeur C, Vatin V, Ghoussaini M, Wachter C, Hercberg S, Charpentier G, Patsch W, Pattou F, Charles MA, Tounian P, Clément K, Jouret B,

.

Weill J, Maddux BA, Goldfine ID, Walley A, Boutin P, Dina C, Froguel P: Variants of ENPP1 are associated with childhood and adult obesity and increase the risk of glucose intolerance and type 2 diabetes. Nature Genet 37: 863–867, 2005.

.

Figure Legends

Fig. 1 The radiograph of the nu/nu mice with bone-metastasized MDA231 cells

Soft X-ray analysis demonstrated the translucent areas meaning osteolytic metastases in the distal metaphyses of femur and proximal metaphyses of tibiae.

Bar: 1cm

Fig. 2 Histological aspects of femur in the nu/nu mice with bone-metastasized MDA231 cells

H-E staining showed the large tumor nest of metastasized MDA231 cells and few fragmented trabeculae in the femoral metaphysis of nu/nu mice **(Fig. 2a, b)**. In this region, a large number of TRAP-positive osteoclasts were located on the scalloped bone surface accumulated abundant osteopontin **(Fig. 2c, d)**. T: tumor nest, ocy: osteocyte

Bars: a: 500μm, b: 250μm, c: 30μm, d: 20μm

Fig. 3 The distribution of FGF23 in the nu/nu mice with bone-metastasized MDA231 cells

The bone-metastasized MDA231 cells revealed intense FGF23 immunoreactivity in tumor nest of nu/nu mice *in vivo* **(Fig. 3b)**, whereas the cultured MDA231 cells showed the no **(arrows)** or faint **(arrowheads)** FGF23 immunoreactivity **(Fig. 3a)**. In the metaphyseal trabeculae of the metastatic region, the osteocytes embedded in the bone matrix didn't exhibit the FGF23 immunoreactivity **(Fig. 3c)**. In contrast, in the distant region from the tumor nest, many FGF23-positive osteocytes could be seen in the bone matrix **(Fig. 3d)**. In the diaphysis, many empty lacunae were present in the superficial layer of cortical bone proximal to tumor nest **(Fig. 3f)**. In the corresponding area, many osteocytes didn't show the FGF23 immunoreactivity **(Fig. 3h)**, while DMP1-positive osteocytes were seen in the cortical bone **(Fig. 3j)**. Note that osteocytes embedded in the cortical bone markedly expressed both FGF23 and DMP1 in control nu/nu mice **(Fig. 3g, i)**.

Bars: a: 10μm, b: 250μm, c: 30μm, e-i: 20μm

.

Fig4. The comparison of serum parameters in the nu/nu mice with bone-metastasized MDA231 cells or subcutaneously injected with MDA231 cells

In the nu/nu mice with bone-metastasized MDA231 cells, serum FGF23 level was significantly increased compared to control (385.87±58.99 vs 155.90±18.17 pg/ml, $p<0.05$) or nu/nu mice subcutaneously injected with MDA231 cells (385.87±58.99 vs 229.65±8.73 pg/ml, $p<0.01$) **(Fig. 4a)**. Serum Ca and Pi didn't show significant difference between all groups **(Fig. 4a)**.

Fig5. Immunolocalization of FGFR1, αklotho, ENPP1, TNALP and PHOSPHO1 in the nu/nu mice with bone-metastasized MDA231 cells

The fibroblastic stromal cells of metastasized tumor nests revealed intense FGFR1 and ENPP1 immunoreactivity in nu/nu mice, whereas the cuboidal tumor cells showed nothing but faint immunoreactivity of FGFR1 and ENPP1**(Fig. 5a, b, d, e)**. Furthermore, the fibroblastic stromal cells expressed faint αklotho immunoreaction in the corresponding area **(Fig. 5c)**. Note that FGFR1- and ENPP1- immunoreactive fibroblastic cells extend their cytoplasmic processes. In contrast, both the fibroblastic stromal cells and cuboitdai tumor cells didn't show TNALP and PHOSPHO-immunopositivity in the tumor nest **(Fig. 5e-i)**. TNALP and PHOSPHO-immunopositivity were observed in osteoblasts located on the trabecular bone surface. T: tumor nest, ocy: osteocyte, tb: trabecular bone

Bars: a-c, g-i: 20μm, d-f: 500μm

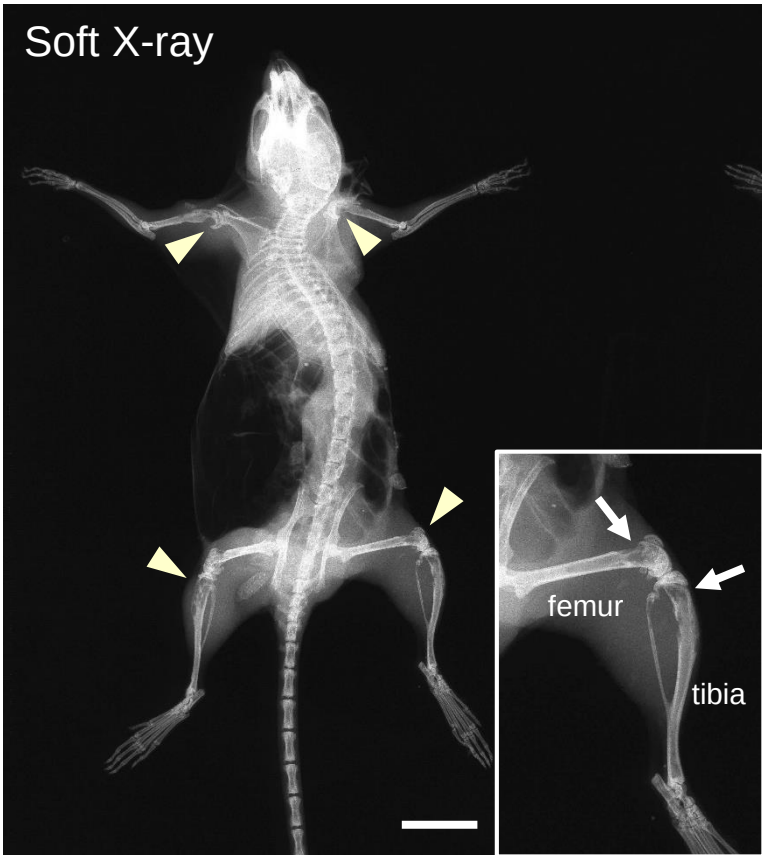

Fig. 1

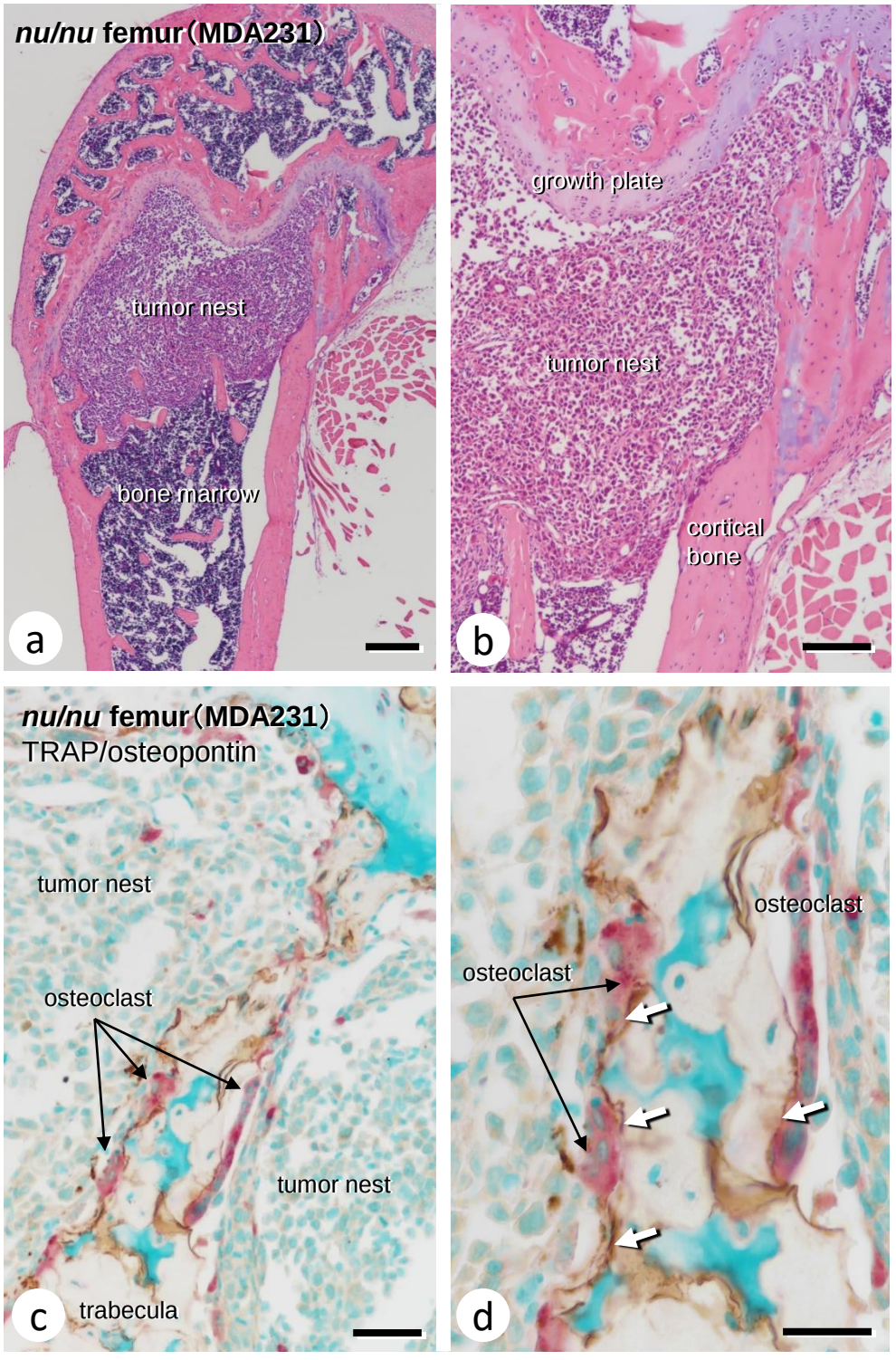
nu/nu femur（MDA231）
tumor nest
bone marrow
a
growth plate
tumor nest
cortical bone
b
nu/nu femur（MDA231）
TRAP/osteopontin
tumor nest
osteoclast
tumor nest
trabecula
c
osteoclast
osteoclast
d

Fig. 2

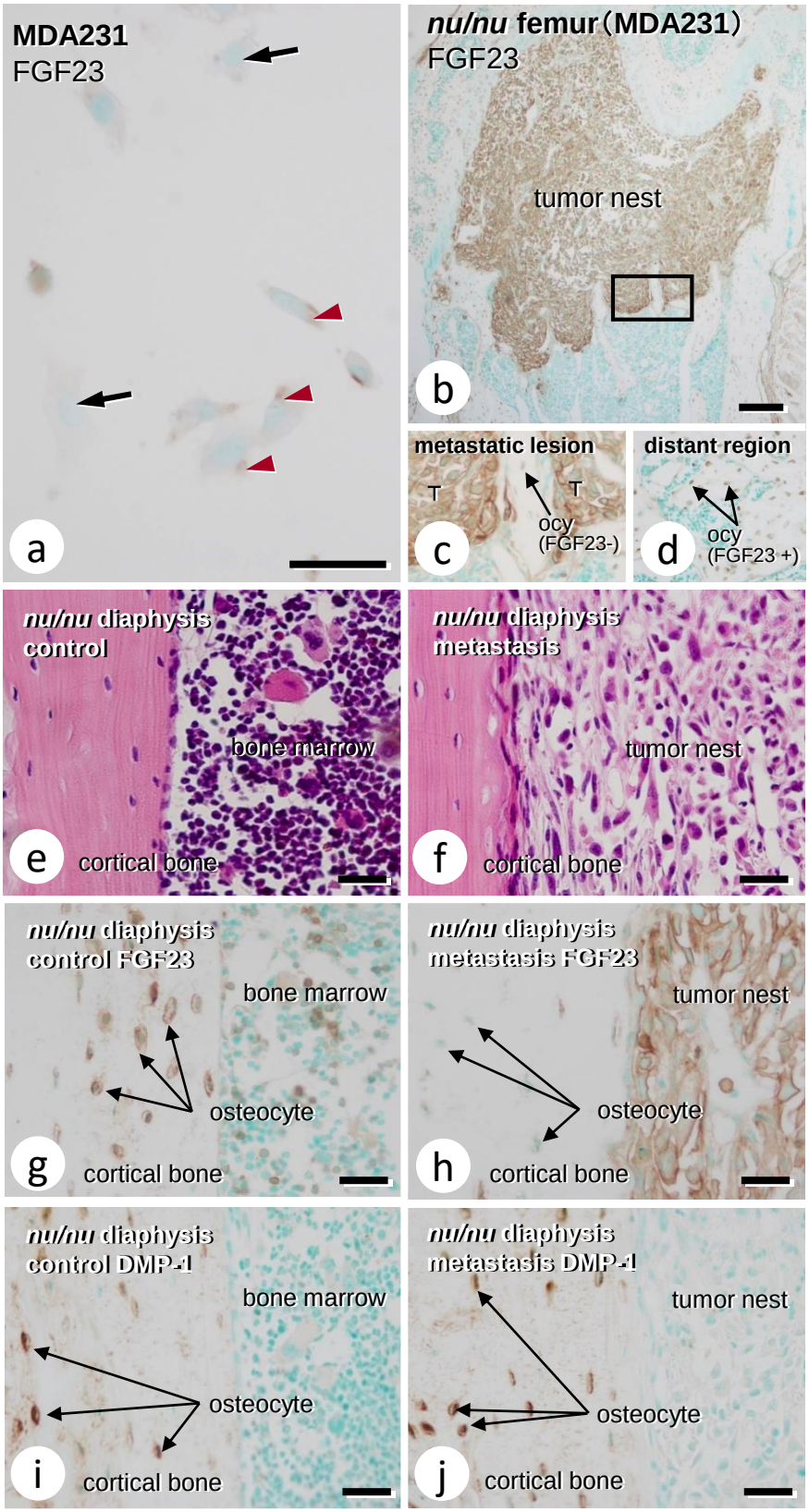
MDA231
FGF23
a
nu/nu femur（MDA231）
FGF23
tumor nest
b
metastatic lesion
T
T
ocy
(FGF23-)
c
distant region
ocy
(FGF23 +)
d
nu/nu diaphysis
control
bone marrow
cortical bone
e
nu/nu diaphysis
metastasis
tumor nest
cortical bone
f
nu/nu diaphysis
control FGF23
bone marrow
osteocyte
cortical bone
g
nu/nu diaphysis
metastasis FGF23
tumor nest
osteocyte
cortical bone
h
nu/nu diaphysis
control DMP-1
bone marrow
osteocyte
cortical bone
i
nu/nu diaphysis
metastasis DMP-1
tumor nest
osteocyte
cortical bone
j

Fig. 3

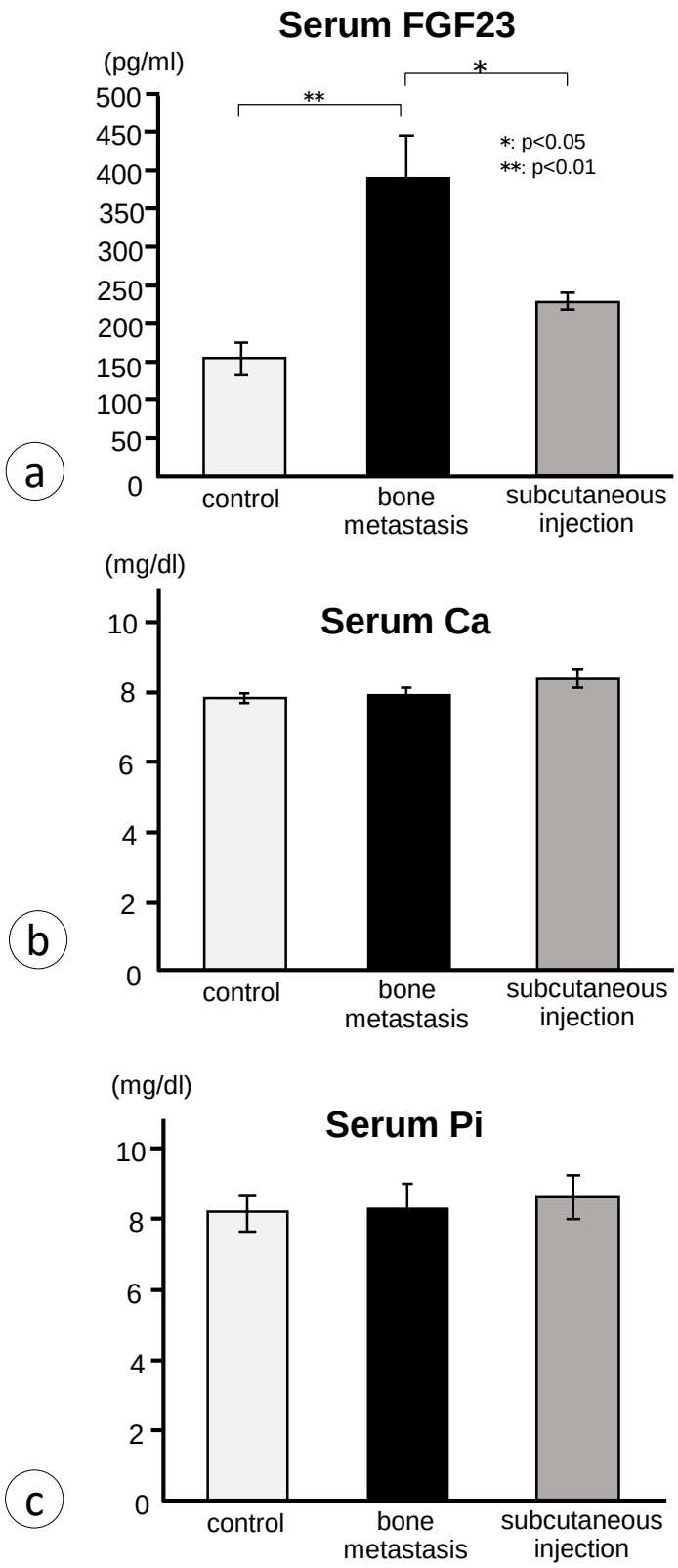
Serum FGF23
(pg/ml)
500
450
400
350
300
250
200
150
100
50
0
**
*
*: p<0.05
**: p<0.01
control
bone metastasis
subcutaneous injection
a
(mg/dl)
Serum Ca
10
8
6
4
2
0
control
bone metastasis
subcutaneous injection
b
(mg/dl)
Serum Pi
10
8
6
4
2
0
control
bone metastasis
subcutaneous injection
c

Fig. 4

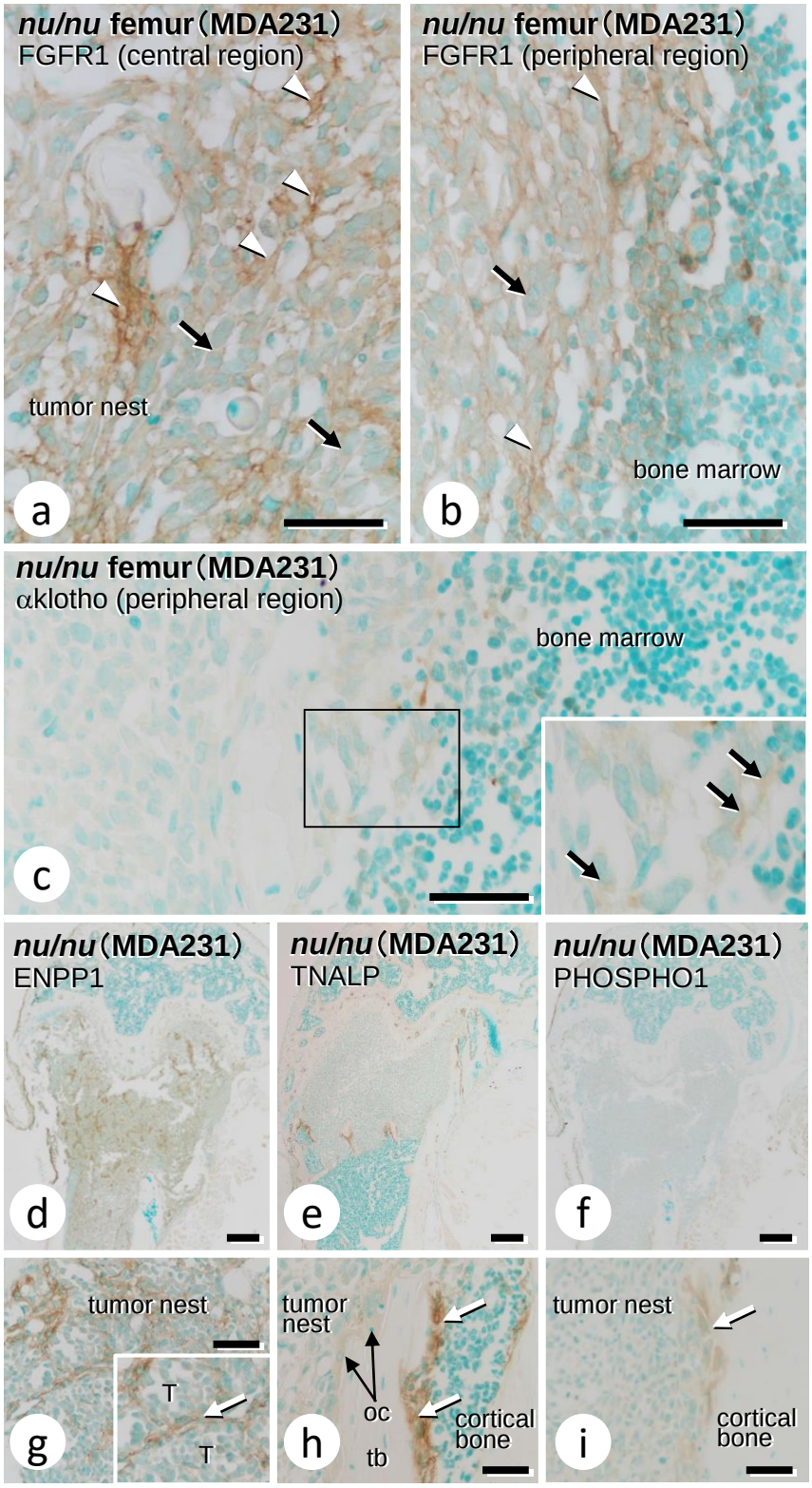
nu/nu femur（MDA231）
FGFR1 (central region)
tumor nest
a
nu/nu femur（MDA231）
FGFR1 (peripheral region)
bone marrow
b
nu/nu femur（MDA231）
αklotho (peripheral region)
bone marrow
c
nu/nu（MDA231）
ENPP1
d
nu/nu（MDA231）
TNALP
e
nu/nu（MDA231）
PHOSPHO1
f
tumor nest
T
T
g
tumor nest
oc
tb
cortical bone
h
tumor nest
cortical bone
i

Fig. 5